

DEVELOPMENT OF A NEW SPECTRAL LIBRARY CLASSIFIER FOR AIRBORNE HYPERSPPECTRAL IMAGES ON HETEROGENEOUS ENVIRONMENTS

A. Mende ^{a, c}, U. Heiden ^b, M. Bachmann ^b, D. Hoja ^c, M. Buchroithner ^a

^a Dresden University of Technology, Institute for Cartography, Dresden, Germany –
andre-mende@web.de, manfred.buchroithner@tu-dresden.de

^b German Aerospace Center, German Remote Sensing Data Center, Wessling, Germany –
uta.heiden@dlr.de, martin.bachmann@dlr.de

^c German Aerospace Center, Remote Sensing Technology Institute, Wessling, Germany –
danielle.hoja@dlr.de

KEYWORDS: Spectral library, SID-SAM mixed measure, Similarity analysis, SLC-Classifier, Statistical reliability measures.

ABSTRACT:

The classification of hyperspectral images on heterogeneous environments without prior knowledge about the study area is a challenging task. Finding potential pure spectral signatures or endmembers (EM) of the various surface materials within an image is essential for obtaining accurate classification results. Automated endmember selection techniques, in many cases, return an unlabelled result without a relationship to a known material.

This study demonstrates the potential of an automated spectral classification approach for hyperspectral imagery by using a comprehensive spectral library including a generalized class structure without the use of prior knowledge of the given scene. The classifier works by comparing every unknown image pixel to all labelled known spectra in the spectral library using a mixed measure similarity analysis of the spectral information divergence SID (Chang, 2000), the spectral angle mapper SAM (Kruse et. al., 1993) and the tangent trigonometric function (Du et. al., 2004). These similarity measures are the main criteria used to assign the class membership to a given pixel. In addition, a statistical analysis of the best ten scores identifies the statistical dominant material class from the similarity analysis. This statistical approach allows a pixel-related estimation of the classification reliability.

The spectral library comparison classifier (SLC-Classifier) enables the classification of hyperspectral images on heterogeneous environments to be as complete as possible (depends on the input spectral library) with results containing both labelled potential pure spectra and spectra with low similarity agreement. Pixels with low similarity agreement are mixed pixels and pixels related to materials without good representative spectra in the comprehensive spectral library. We demonstrate that this classifier is suitable for the identification of surface materials using hyperspectral images where detailed knowledge about the environments does not exist.

1. INTRODUCTION

Many hyperspectral images contain both natural and anthropogenic surface materials. In most cases there is no in-situ knowledge about the different surface materials and their related spectral variability. Every supervised classification needs a representative and well-prepared training dataset for all important material classes within the image. The quality of the classification result depends on the quality of the image-related training dataset and the skill of the user, or expert, who determines the training datasets. Therefore, training datasets from different users will typically not produce comparable classification results.

The challenge in developing a good classification method is including spectral characteristics of different material classes. From this it follows that comprehensive classification approaches should contain full knowledge about the spectral characteristics and absorption features of all relevant material classes. One possible solution to deliver spectral characteristics of known material classes to a classification approach is the use of a comprehensive spectral library of image spectra as a training database. Additionally, the spectral library of image spectra enables the requirement of the comparableness of several classification results for different test sites.

Research objectives

The objective of this study is to develop a classifier that is able to identify natural and anthropogenic surface materials without local spectral knowledge of the hyperspectral image of interest. The idea is to use a comprehensive and well structured hyperspectral library of image spectra containing a wide range of predominantly anthropogenic materials (in urban areas) and key representatives of the natural surfaces (being aware of the high spectral variability of vegetation). A suitable comparison measure must be chosen to compare each image pixel spectra to the known image spectra of the comprehensive spectral library. Finally, the combination of various information layers enables the identification of EMs that are subsequently used to derive an area-wide classification of a hyperspectral image and to assess the reliability of the classification results. Issues that must be addressed using this approach include the incompleteness of the spectral library and mixed pixels.

2. DATA BASE

2.1 Spectral library of image spectra

In this study a comprehensive and well structured spectral library is used. The spectral library contains 5,890 spectra comprising 36 different material classes. The spectra of the library are derived from HyMap imagery from four different test sites in Germany: Berlin, Potsdam, Dresden and Munich (Roessner et. al., 2011; Heldens et. al., 2008 and Heiden et. al., 2007). The requirement of consistent pre-processing and atmospheric correction for the compiled spectral library was ensured by using the process chain of the DLR (Bachmann et. al., 2007) and ATCOR (Richter, 2010). The spectral library includes predominantly a wide range of known anthropogenic materials and their within-class spectral variations. Natural materials in the spectral library are included using representative spectra, because of their high spectral variability. This study shows that we are able to deal with the low number of representative natural spectra and the incompleteness of the spectral library. The number of spectra for the different material classes should be uniformly distributed with the requirement that all thematic library classes form a consistent class hierarchy. Additionally, the number of meaningful spectra representing each class becomes an important issue as it is useful to describe every material class with all possible characteristics and related within-class spectral variability. However, the goal here is not to include every possible spectral variation, but only those that are necessary. A consistent and well-structured class hierarchy (Anderson et. al., 1976; Heiden et. al., 2007) of the spectral library is necessary to be comparable to other classification approaches or to be able to use different generalization levels for an application. Five different generalization levels are defined for the class hierarchy of the spectral library. The requirement of the class hierarchy is to be able to sum up every detailed material class to thematic main classes using different generalization levels. The main type stands for the highest generalization level (level 1) and the surface material instance (level 5) contains a number of instance spectra which represents the within-class variations of surface materials due to e.g. different coating or colours characterisations. The surface materials (level 4) are relevant for the interpretation and the visualization of the classification results of this paper.

Generalization level	Generalization name	Example
Level 1	Main types	Anthropogenic / artificial surface
Level 2	Land cover types	Building / roofs
Level 3	Material types	Metallic materials
Level 4	Surface materials	Aluminium
Level 5	Surface material instances	Aluminium Instance No. 10

Table 1: Basic class hierarchy structure of the input spectral library.

2.2 Hyperspectral image data

To demonstrate the reliability of the SLC-Classifer, a test site in France (Mende) was chosen, because of the differing material occurrences of special material classes (e.g. roof tile) between German cities (used for creating the spectral library) and the French town Mende (Fig. 5). The spatial resolution of the test site is $4\text{ m} \times 4\text{ m}$ covering the reflective part of the electromagnetic spectrum in 125 channels ($0.45\text{ }\mu\text{m} - 2.5\text{ }\mu\text{m}$) of the HyMap airborne sensor. The size of the test site subset is $1,204\text{ m} \times 1,204\text{ m}$ and was corrected for radiometric artefacts, atmospherically corrected with ATCOR (Richter, 2010) and geometrically corrected with ORTHO (Müller et. al., 2005).

3. METHODS

3.1 Spectral similarity analysis

The SLC-Classifer uses a similarity analysis of each pixel spectrum of the image compared to all spectra in the spectral library. This analysis is based on the SID-SAM mixed measure (Du et. al., 2004), which is calculated by multiplying SID (Chang, 1999 and Chang, 2000) by the tangent of SAM (Kruse et. al., 1993) between the *spectral pixel signature* s and *spectral library signature* s' .

$$SID(TAN) = SID(s, s') \times \tan(SAM(s, s')) \quad (1)$$

The effect of this combined measure of SID and SAM in Eq. (1) will be a better discriminability of the numerical similarity representation of SAM and SID. SAM is almost insensitive to the overall brightness and SID is an improved measure for spectral similarity between two spectral signatures using the probabilistic discrepancy (Chang, 2000). The $SID(TAN)$ value of two similar spectra will be closer and of two dissimilar spectra will be more distinct (Du et. al., 2004). The SLC-Classifer ranks all the similarity values for each pixel and stores the best similarity value in an additional image (Fig. 4). For two identical spectra the $SID(TAN)$ value will be zero.

3.2 Best similarity value classification

The $SID(TAN)$ similarity measure is the main criterion to assign the class membership of the considered pixel. Therefore, every pixel in the image will be assigned to the material class with the highest similarity agreement. The target class is defined as the material

class with the highest similarity agreement for the given pixel. For pixel-related reliability estimations an advanced system of rules is implemented for the SLC-Classifier: the weighted score occurrence, the statistical dominant material class and the albedo. The classification results for the best similarity value classification are shown in Fig. 3.

3.3 Weighted score occurrence

Using the pixel-related *weighted score occurrence* $p_{(target\ class)}$ of the target class an estimation of the statistical reliability can be conducted. The *target class* is defined as the material class of the best ranked similarity value for the given pixel. All different material classes which occur in the best ten ranked similarity values are called *score classes* for the given pixel. The target class is one of the score classes. The range of $p_{(target\ class)}$ is between zero and one hundred percent. Values near one hundred percent are a good indicator of a reliable classification. Low values show that one or more additional material classes were scored in the best ten ranked similarity values and the classification result for the given pixel could be inaccurate.

The weighted score occurrence is the first reliability calculation of this study and is finally defined in Eq. (5). It uses a statistical analysis of the best ten scores of the similarity analysis for a given pixel. For this analysis the target class will be defined as the class related to the best similarity value using Eq. (1). The algorithm counts the *number of times the target classes scores in the best ten similarity values* stored in $n_{(score\ class\ x = target\ class)}$. The same will be done for all other *score classes* and stored in $n_{(score\ class\ x)}$. The reason for applying weights for the statistical analysis is based on the requirement that all material classes should have the same number of spectra in the spectral library. If a material class has more spectra than a spectrally similar, but thematic different class, then the classification probabilities will not be equal and the results not representative. For the calculation of the weights using Eq. (2) the material class from the best ten similarity values with the largest number of spectra in the spectral library will be used to store the related number of library spectra as the variable $n_{(max)}$. The pixel-related score class weights will be calculated for each pixel and for all scored classes. All other *number of spectra of each scored classes* $n_{(score\ class\ x)}$ will be scaled with a *material class-related linear weight* $w_{(score\ class\ x)}$ from $n_{(score\ class\ x)}$ up to $n_{(max)}$.

$$w_{(score\ class\ x)} = \frac{n_{(max)}}{n_{(score\ class\ x)}} \quad (2)$$

Based on Eq. (2) the pixel-related *weighted score occurrence* $p_{(target\ class)}$ of the target class Eq. (5) will be calculated in percentage as a statistical measure of the classification reliability of the given pixel. This is the ratio of the *weighted number of scores of the target class* $n^*_{(weighted\ number\ of\ score\ class = target\ class)}$ and the *sum of the weights multiplied with the related number of scores* $s^*_{(weights\ of\ best\ ten\ scores)}$ of the best ten scores of the similarity values.

$$n^*_{(weighted\ number\ of\ score\ class\ x = target\ class)} = n_{(score\ class\ x = target\ class)} \times w_{(score\ class\ x = target\ class)} \quad (3)$$

The variable $n^*_{(weighted\ number\ of\ score\ class\ x = target\ class)}$ is calculated by multiplying the *number of target class scores* $n_{(score\ class\ x = target\ class)}$ and the related *weight of the target class* $w_{(score\ class\ x = target\ class)}$ (Eq. 4). This calculation will be done for all score classes. The *number of different scored material classes* for the considered pixel is stored as k .

$$s^*_{(weights\ of\ best\ ten\ scores)} = \sum_{x=1}^k n_{(score\ class\ x)} \times w_{(score\ class\ x)} \quad (4)$$

The pixel-related calculation Eq. (4) of $s^*_{(weights\ of\ best\ ten\ scores)}$ is defined with *summed multiplication of all counted scores of the different score classes* $n_{(score\ class\ x)}$ and the *class-related linear score class weight* $w_{(score\ class\ x)}$.

$$p_{(target\ class)} = 100 \times \frac{n^*_{(weighted\ number\ of\ score\ class = target\ class)}}{s^*_{(weights\ of\ best\ ten\ scores)}} \quad (5)$$

An example of the pixel-related weighted score occurrence calculation is shown in Fig. 1. In this example an image pixel is classified as a “concrete” material based on the best similarity value (column 2). The column labelled “class relationship” contains the name of the scored class and which spectrum from the spectral library was referenced. The number of scores of the target class “concrete” is eight of ten. The spectral library comprises 120 “concrete” and 60 “asphalt” spectra with individual weights for the two classes calculated using Eq. (2).

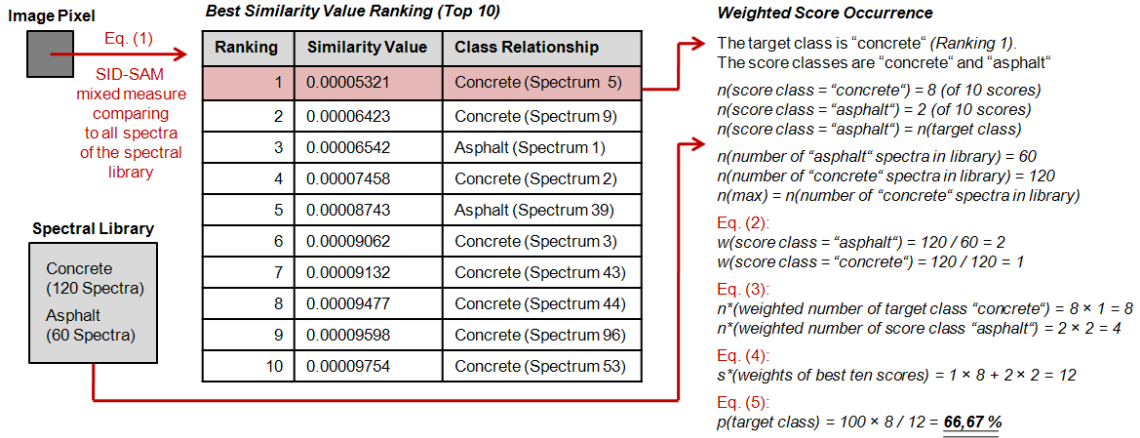


Figure 1: Calculation of the weighted score occurrence of a given pixel.

3.4 Statistical dominant material class

The weighted score occurrence Eq. (5) allows for the estimation of the statistical reliability for the best similarity value classification assignment of the given pixel. The statistical analysis of the ten best ranked similarity values can also be used for finding the statistical dominant material class if the weighted score occurrence value is under fifty percent. This special case usually occurs for noisy and mixed pixels where two different classes with nearly the same spectral characteristics look similar to the pixel. Another case could occur if a pixel spectrum is similar to two different material classes that are themselves spectrally similar. The calculation of the statistical dominant material class of the best ten ranked similarity values provides the second reliability calculation of the SLC-Classifier. It will be calculated with Eq. (5) by using the material class with the highest value of the *weighted number of scores of the target class* n^* (weighted number of score class = target class) Eq. (3) analysing the best ten ranked similarity values. The statistical dominant material class in that case could differ from the best similarity value class. The results of the statistical dominant material class for the test site are represented in Fig. 3.

3.5 Albedo

The third reliability test calculates the ratio between the mean albedo of the reference spectrum and mean albedo of the pixel spectrum. For some material classes the overall albedo of the spectrum represents a key spectral characteristic that distinguishes that class. For example, the difference in albedo becomes the main criterion to differentiate two spectral similar materials. Therefore, it is useful to calculate for each classified pixel the *albedo ratio* $a(s, s')$ between the given *mean albedo of the pixel spectrum* s' and *mean albedo of the most similar library spectrum* s .

$$a(s, s') = \frac{s'}{s} \quad (6)$$

If the result of Eq. (6) is $\gg 1$ (much brighter) or $\ll 1$ (much darker) the classification reliability could be poor for the given materials. The albedo ratio can be used as a knowledge-based indicator of the quality of the classification results (Fig. 4). In the case of noisy pixels the albedo ratio value for a given pixel would be much brighter (Fig. 4 right: the white spatial cluster) than the reference spectrum of the spectral library.

3.6 Incompleteness of the spectral library

The SLC-Classifier has the ability to deal with the incompleteness of the spectral library. The similarity measure of Eq. (1) stores the best ranked similarity value with the related material class for each pixel. However, it is also possible to determine those spectra with the worst similarity measures. These spectra may potentially define important spectra that are missing from the original spectral library. Finding those spectra with the worst similarity measures requires a meaningful similarity threshold. Therefore, a statistical acceptance was chosen that one percent of the image pixels are considered incorrectly classified. The one percent threshold is based on the empirical experience that a comparable classification approach has a much lower accuracy than ninety-nine percent. The pixels which are included in the one percent poorly classified boundary will be used as a new training dataset of spectra stored in an additional spectral library. Underrating the one percent poorly classified number of pixels will be reasonable because of an additional similarity analysis Eq. (1) of the image using the new training dataset of the one percent containing pixels. Every image pixel has the opportunity being more similar to one spectrum of the new training dataset than to classification iteration with the spectral library. After this calculation the one percent training dataset will grow up to a multiple of the number of poorly classified pixels. The classification result will not change, but the calculation of the poorly classified pixel analysis results in an output mask of poorly classified pixels (Fig. 5) representing the mixed pixel problem.

4. RESULTS AND DISCUSSION

4.1 Distribution of the best similarity values of all pixels for the test site image

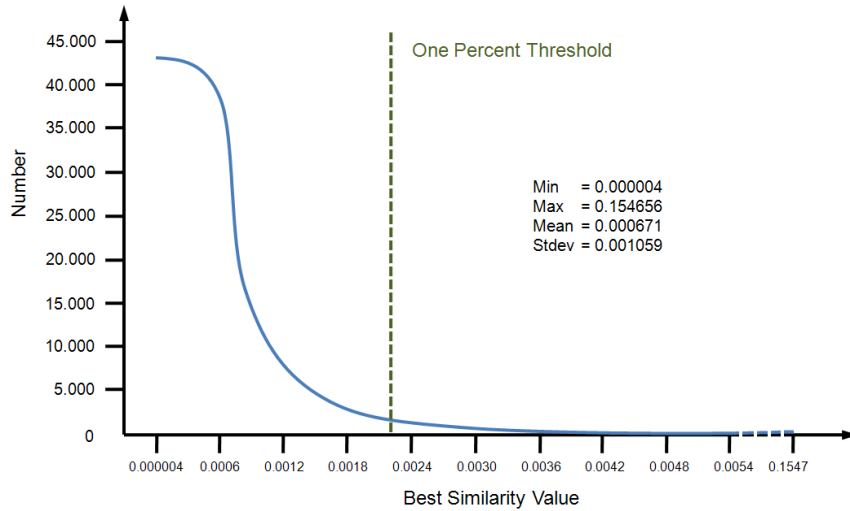


Figure 2: This plot shows the distribution of the best similarity values for the test site (90,601 pixels). The vertical line (green) shows the similarity threshold which was used as an additional spectral library of poorly classified spectra.

The distribution of the ranked similarity values calculated with Eq. (1) shows that a large number of pixels have a high similarity value. The border between high similarity values (“pure pixels” having a value near zero) and low similarity values (likely “mixed pixels”) is not separable numerically. The worst similarity values near 0.1547 shown in Fig. 2 represent noisy pixels.

4.2 Classification result and statistical indicators for reliability estimation

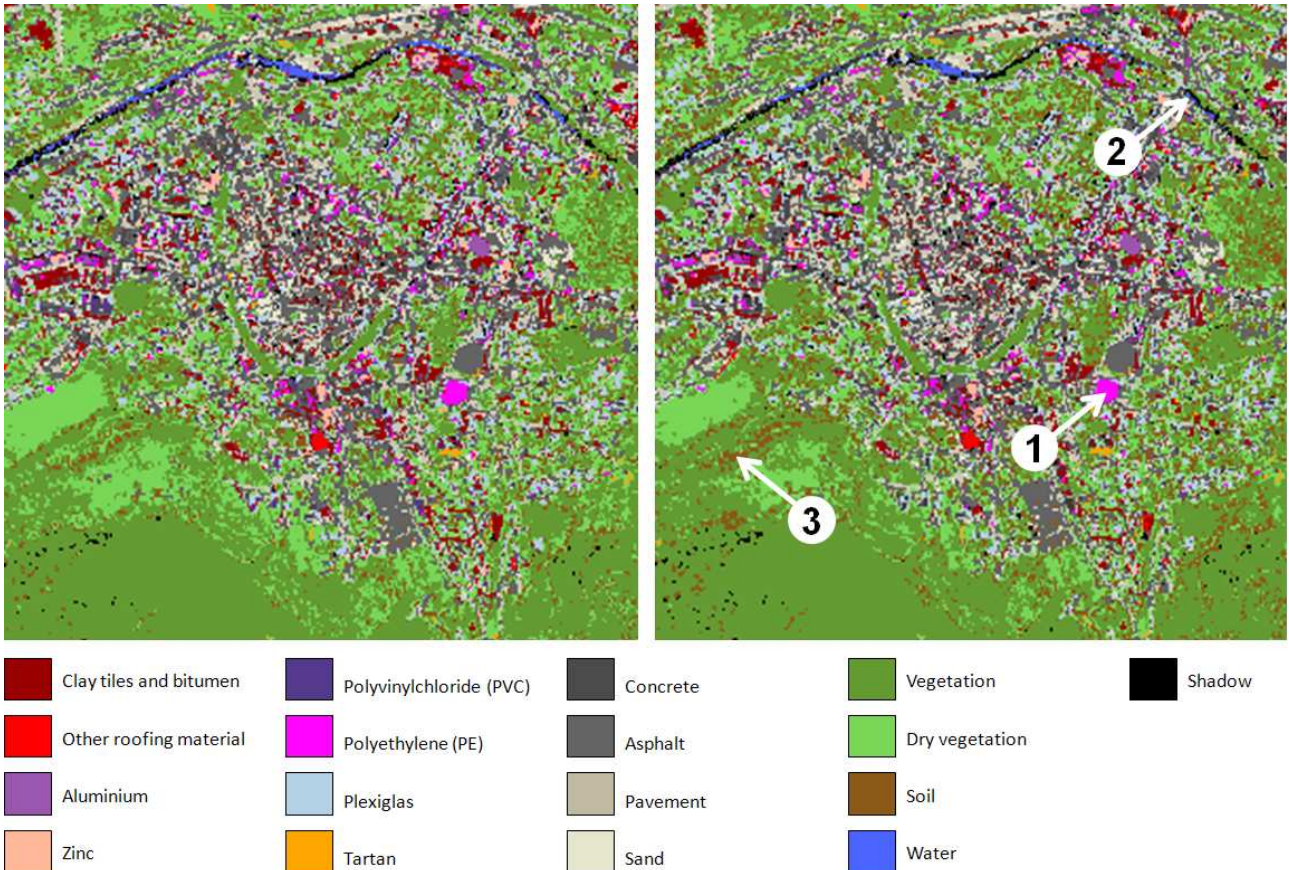


Figure 3: Classification results for the best similarity value (left) and the statistical dominant material class (right).

The two classifications look almost same which stands for a good reliability of the results. Natural materials (e.g. vegetation) are good represented, although only representative spectra are included in the used spectral library. The artificial materials of the image are well-classified and sealed urban structures can be detected (e.g. polyethylene Fig. 3 arrow 1).

Comparing the classification results for the best similarity value and the statistical dominant material class the greatest differences appear for the classes “water/shadow” (Fig. 3 arrow 2) and “dry vegetation/soil” (Fig. 3 arrow 3). “Water” and “shadow” often are confused in the classification image, which is expected as they both have very low albedo. “Dry vegetation” is also a challenge as it is often a mixed class containing “vegetation” and some degree of background “soil”. Therefore, the spectral signature of “dry vegetation” is similar to “vegetation” and “soil”, with differences only in small absorption features. From this it follows that the input spectral library does not represent the spectral variability within the test area and should be revised to improve classification results.

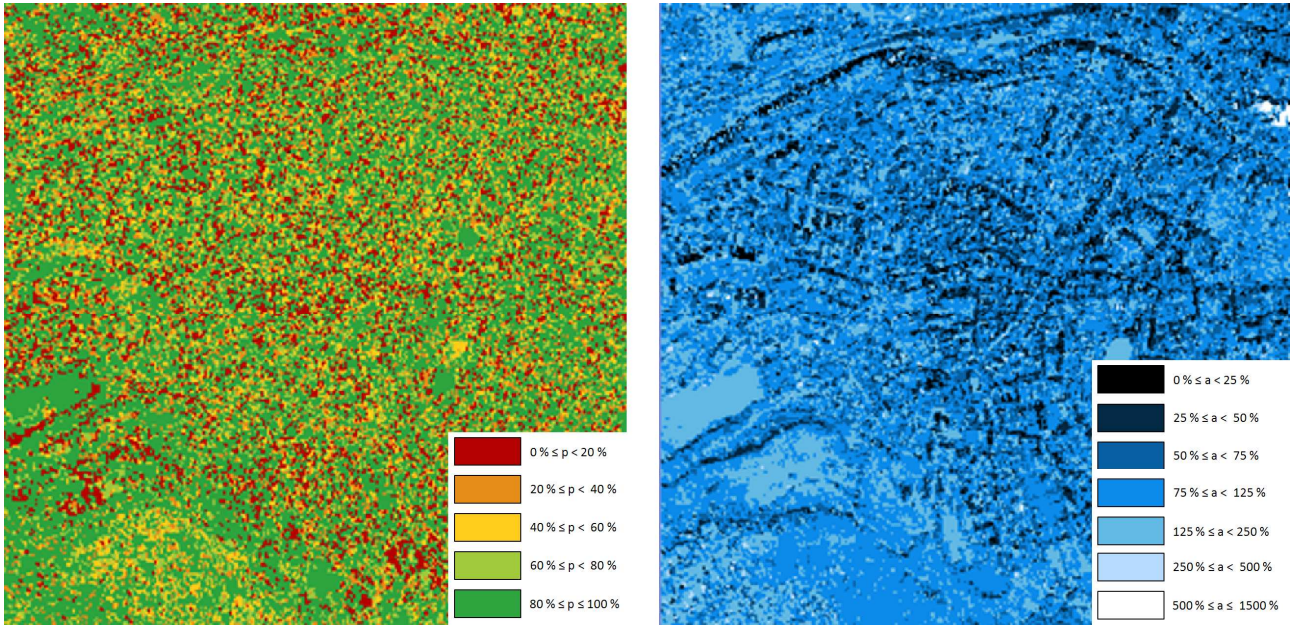


Figure 4: The weighted score occurrence (left) and the albedo ratio (right) for the test site image. The albedo ratio values Eq. (6) are multiplied with one hundred to scale them to percentage.

Weighted score occurrence	
Class range	Distribution
$0 \% \leq p < 20 \%$	14.5 %
$20 \% \leq p < 40 \%$	11.8 %
$40 \% \leq p < 60 \%$	9.3 %
$60 \% \leq p < 80 \%$	11.5 %
$80 \% \leq p \leq 100 \%$	52.9 %

Albedo ratio	
Class range	Distribution
$0 \% \leq a < 25 \%$	4.0 %
$25 \% \leq a < 50 \%$	12.8 %
$50 \% \leq a < 75 \%$	24.7 %
$75 \% \leq a < 125 \%$	40.1 %
$125 \% \leq a < 250 \%$	7.8 %
$250 \% \leq a < 500 \%$	0.5 %
$500 \% \leq a \leq 1500 \%$	0.1 %

Table 2: These tables show the percentage class distribution of both images of Fig. 4.

To estimate the reliability of the classification the weighted score occurrence using Eq. (5) was calculated and is shown in Fig. 4. Table 2 shows that the majority of the pixels have a good statistical reliability of the weighted score occurrence. The lower the weighted score occurrence of a pixel (red in Fig. 4, 14.5 % of the image) the greater the probability of confusion between two or more similar material classes. Therefore, this measure is a good indicator for the statistical reliability of the classification result. A low weighted score occurrence could also be caused by the incompleteness of the spectral library. If the spectral library has not enough representative spectra of a material class then the weighted score occurrence value is not representative. A high value of the weighted score occurrence represents a good classification reliability (dark green in Fig. 4, 52.9 % of the image) if the best similarity value of the pixel is near the statistical minimum (Fig. 2).

Using the albedo ratio as a reliability measure for the discrimination of spectrally similar material classes is meaningful. In some cases the albedo is the only distinguishing characteristic between two similar classes. A material-related albedo ratio threshold could be an opportunity to estimate the reliability of the classification result. For example, spectral similar material classes like “concrete” and “asphalt” which mainly can differentiate using the albedo. The black coloured class range ($0 \% \leq a < 25 \%$) represents mainly shadowed pixels. The class range ($500 \% \leq a \leq 1500 \%$) coloured in white shows pixels with specular reflectance characteristics. A

large part (40.1 %) of the image pixels were classified using a reference spectrum with a low deviation of the albedo ratio, shown in Table 2.

The two tables show that the used spectral library is well-prepared for classifying the majority of the images pixels for this test site and the reliability measures enables the validation of the classified pixels.

4.3 Poorly classified pixel mask

The poorly classified mask (Fig. 5, left) is the result of the one percent rule (Fig. 2) and an additional iteration of the similarity analysis Eq. (1). Using the one percent rule 906 pixels are retained as a training database with the additional iteration of the similarity analysis growing the mask to 17,485 pixels (representing 19.29 % of the test site). It shows spatial clusters of similar materials which are not well-represented in the spectral library. Mainly vegetation, soil and water pixels are included in the poorly classified pixel mask. The low number of urban pixels in the poorly classified pixel mask shows that the spectral library is well-prepared for anthropogenic materials. A manual analysis of the spatial clusters was done and examples of the resulting spectra from this manual analysis are shown in Fig. 6.

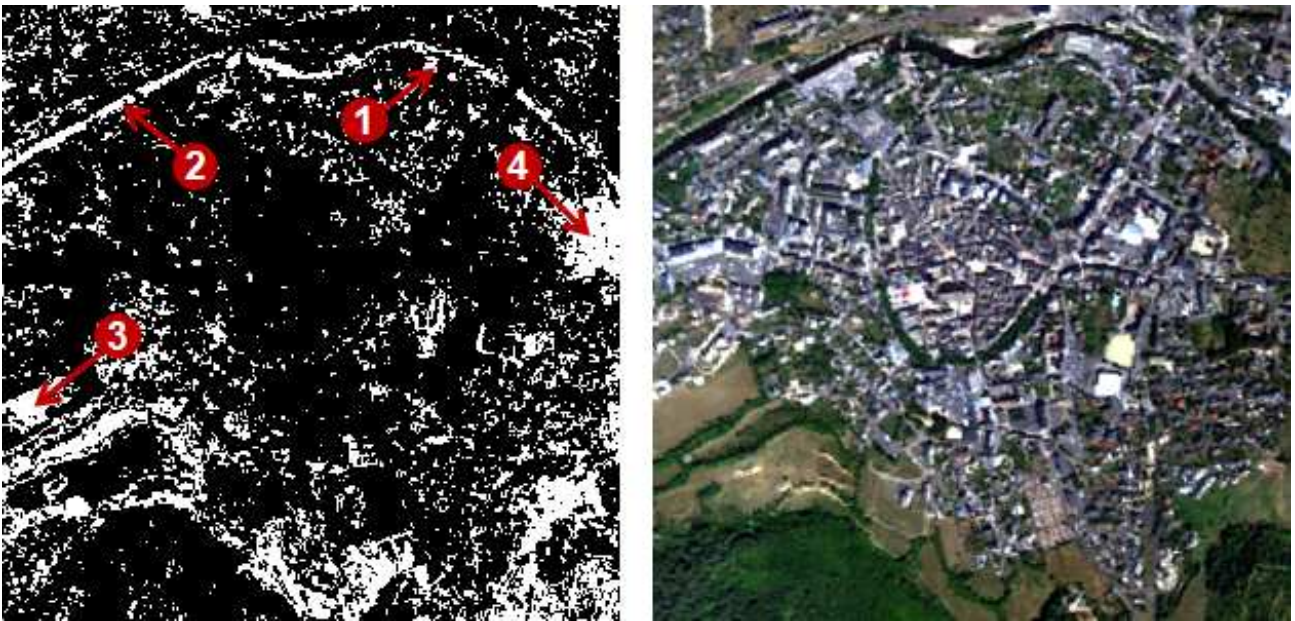


Figure 5: The mask (left) shows the distribution of the pixels with the lowest similarity values using the one percent rule and the similarity analysis from Eq. (1). The RGB-Image (right) shows the true colour image of the test site. The locations of four different poorly classified pixels are marked and represented in Fig. 6.

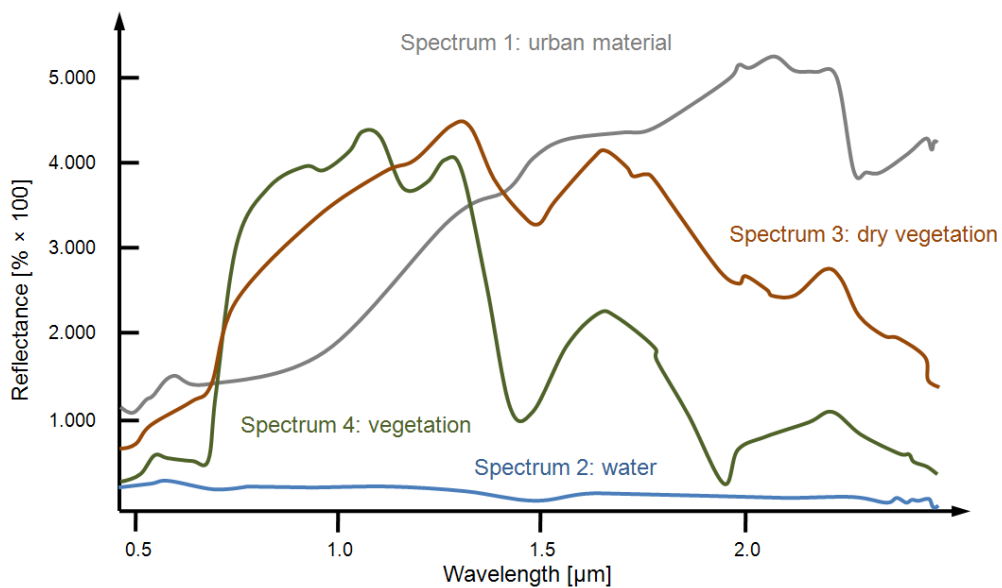


Figure 6: Spectral signatures of four different pixels derived from the poorly classified pixel mask.

As expected a large number of mixed pixels are contained within the mask. However, new material classes occurring as spatial clusters, which are not included in the spectral library, are included in the mask (Fig. 6 cp. spectra 1). In addition, if the spectral variability of one material is not representative for the given test site, the mask will contain spatial clusters of the material class with a deviation relative to the spectral characteristics to the scored class spectrum (Fig. 6 cp. spectra 2, 3, 4). The main finding is that not only mixed pixels are included in the mask but also pure pixels representing material classes which are not included or underrepresented in the spectral library. Therefore, this mask forms the basis for improving of the spectral library, such that missing material classes or poor representatives of spectral class variability can be dealt with and the disadvantages of an incomplete spectral library of image spectra can be minimized.

5. CONCLUSION

The classification results demonstrate the potential of the SLC-Classifier to classify natural and anthropogenic surfaces. This is accomplished by using the similarity analysis of the SID-SAM mixed measure and additional reliability calculations.

The biggest challenges of developing the SLC-Classifier were to deal with the incompleteness of the spectral library, to find criteria and indicators for the improvement of the spectral library and to develop a reliability analysis to estimate the classification results. The final result contains the classification, the reliability analysis and pixel-related statistical measures. This allows the SLC-Classifier to consider pure and mixed pixels and within-class spectral variability of surface materials. Additionally, the poorly classified mask potentially can be used to improve the spectral library by highlighting missing material spectra and thus, subsequent classifications. The challenge for the user is to decide whether to include the new spectra in the spectral library or to use a spectral library of local image spectra to improve the current classification results. It is important that the spectral library includes only those spectra that are necessary, rather than trying to include every possible spectral variation.

Because of the different reliability measures and the consistent class hierarchy of the spectral library, it is possible to compare the classification results of the SLC-Classifier with other classification results of different classifiers or to be integrated in an ensemble classification approach. The study shows that a comprehensive spectral library can be used as a quality training database for classifying unknown hyperspectral images of heterogeneous environments without prior knowledge about the test site. In addition, the use of the SLC-Classifier as an EM extraction technique is possible if the operator defines a decision tree of meaningful thresholds using all information layers.

6. OUTLOOK

The greatest potential of the improvement of the SLC-Classifier exists for the treatment of the incompleteness of the spectral library. The mask of potential poorly classified pixels can be used to estimate the incompleteness of the spectral library. The user can use this poorly classified mask to search for spectral and spatial clusters containing material classes which are currently not included in the spectral library. At this point the user has to decide whether a possibly missing spectrum should be included into the spectral library or not. A meaningful solution could be to distinguish both a spectral library containing a large number of comprehensive material classes and a spectral library of local image spectra which includes image-related spectra without representative spectral characteristics for improving the reliability of the current classification result.

A major challenge with hyperspectral imagery is to identify pure pixels within the given scene. With the estimation algorithms and different statistical reliabilities, the SLC-Classifier could potentially allow it to be used for EM detection using hard thresholds for all information layers. For example, the potential for an EM is very high if the best similarity ranked class is equal to the statistical dominant material class and the weighted score occurrence (Fig. 4 cp. class range: $80 \% \leq p \leq 100 \%$) is near one hundred percent. Additionally, the best similarity value should be near to the minimum value of the best ranked similarity values (Fig. 2) and deviation of the albedo ratio should be low (Fig. 4 cp. class range: $75 \% \leq a < 125 \%$). With threshold values set or a decision tree for the above factors it would be possible to generate a potential pure pixel mask that subsequently could be used to define EMs for unmixing.

7. REFERENCES

- Anderson, J. R., Hardy, E. E., Roach, J. T., Witmer, R. E., 1976. A Land Use and Land Cover Classification Scheme for Use with Remote Sensor Data. U.S. Geological Survey.
- Bachmann, M., Habermayer, M., Holzwarth, S., Richter, R., Müller, A., 2007. Including Quality Measures in an Automated Processing Chain for Airborne Hyperspectral Data. In: 5th EARSeL Workshop on Imaging Spectroscopy. EARSeL-SIG-IS 2007, Bruges, Belgium.
- Chang, C.-I., 1999. Spectral information divergence for hyperspectral image analysis. In: Geoscience and Remote Sensing Symposium, 1999. IGARSS '99 Proceedings. IEEE 1999 International, Vol. 1, pp. 509 – 511.
- Chang, C.-I., 2000. An Information-Theoretic Approach to Spectral Variability, Similarity, and Discrimination for Hyperspectral Image Analysis. In: IEEE Transactions on Information Theory, Vol. 46, No. 5.
- Du, Y., Chang, C.-I., Ren, H., Chang, C.-C., Jensen, J. O., 2004. New hyperspectral discrimination measure for spectral characterization. In: Optical Engineering, Vol. 43, No. 8.

- Heiden, U., Roessner, S., Segl, K., Kaufmann, H., 2007. Determination of robust spectral features for identification of urban surface materials in hyperspectral remote sensing data. In: Remote Sensing of Environment, Vol. 111, Issue 4.
- Heldens, W., Esch, T., Heiden, U. and Dech, S., 2008. Potential of hyperspectral remote sensing for characterisation of urban structure in Munich. In: Remote Sensing - New Challenges of High Resolution, pp. 94 – 103. EARSeL Joint Workshop Bochum.
- Kruse, F. A., Lefkoff, A. B., Boardman, J. W., Heidebrecht, K. B., Shapiro, A. T., Barloon, P. J. and Goetz, A. F. H., 1993. The Spectral Image Processing System (SIPS) – Interactive Visualization and Analysis of Imaging Spectrometer Data. In: Remote Sensing of Environment, Vol. 44, pp. 145 – 163.
- Müller, R., Lehner, M., Reinartz, P., Schroeder, M., 2005. Evaluation of spaceborne and airborne line scanner images using a generic ortho image processor. Commission I, WG I/5, DLR, Wessling, Germany.
- Richter, R., 2010. Atmospheric / topographic correction for airborne imagery: ATCOR-4 User Guide. DLR-IB 565-02/10. Wessling, Germany.
- Roessner, S., Segl, K., Bochow, M., Heiden, U., Heldens, W. and Kaufmann, H., 2011. Potential of hyperspectral remote sensing for analyzing the urban environment. In: Urban Remote Sensing: Monitoring, Synthesis and Modeling in the Urban Environment Wiley-Blackwell (in press), pp. 49 – 61.